Thermodynamic Study of Phase Transitions in Lyotropic Systems: Adiabatic Calorimetry on Nonionic Surfactant $C_{16}E_8$−Water System†

Kazuya Saito,* Noriaki Kitamura, and Michio Sorai

Research Center for Molecular Thermodynamics, Graduate School of Science, Osaka University, Toyonaka, Osaka 560-0043, Japan

Received: February 26, 2003

Heat capacities of the binary systems consisting of a nonionic surfactant $C_{16}E_8$ and water were precisely measured as a function of temperature by adiabatic calorimetry over the temperature and the concentration ranges where lyotropic liquid crystals are formed. The enthalpy and entropy of transitions were determined for all known phase transitions observed. Comparison of the present result and the previous one on the $C_{12}E_6$−water system suggests that the higher order structure in the liquid crystalline phases in these systems be mainly constructed by surfactant molecules with a fixed amount of water. The excess heat capacities, as estimated by measuring the heat capacity of neat $C_{16}E_8$, are positive over the whole temperature and concentration ranges. Properties of lyotropic and thermotropic systems are compared briefly, while attention is given to the geometries of surfaces characterizing the aggregation (triply periodic minimal surface for cubic phases and flat surfaces for lamellar and smectic phases).

1. Introduction

Amphiphilic molecules having both hydrophilic and hydrophobic parts form lyotropic liquid crystals in the presence of water. The representative aggregation states with translational order are lamellar phases with one-dimensional (1D) periodicity (neat phases), hexagonal phases with two-dimensional (2D) periodicity (middle phases, often with space group *p*6*m*), and cubic phases with three-dimensional (3D) periodicity (often with space group *Ia*3*d*).[1,2] The type of mesophase observed in these lyotropic systems can be explained using an interfacial curvature, which depends on the shape of hydrated surfactant molecule characterized by surfactant parameter.[3] Various studies have extensively been carried out on such systems to see the transformation of one structure into another. Of these, most thermodynamic studies are based on a traditional view of solution thermodynamics. Little has been discussed from the view of mechanism of structure building accordingly.

In a previous paper,[4] the heat capacities of the binary systems consisting of a nonionic surfactant hexaoxyethylene−*n*-dodecyl ether [*n*-$C_{12}H_{25}(OCH_2CH_2)_6OH$, abbreviated as $C_{12}E_6$ or $C_{12}EO_6$] and water, and that of neat $C_{12}E_6$ were precisely measured as a function of temperature by adiabatic calorimetry. The enthalpy and entropy gains at the phase transitions between liquid crystalline phases were essentially constant if compared per mole of $C_{12}E_6$ basis, which is a natural unit from the view of mechanism of structure building. The excess heat capacities were estimated to be positive over the whole temperature and concentration ranges. The excess heat capacities of two liquid crystalline phases show "master curves" if compared per mole of $C_{12}E_6$ basis. These findings were correlated to the idea that the higher order structure in the liquid crystalline phases in this system is mainly built by $C_{12}E_6$ molecules with a fixed amount of water.

The present binary system of the nonionic surfactant octaoxyethylene−*n*-hexadecyl ether [*n*-$C_{16}H_{33}(OCH_2CH_2)_8OH$, abbreviated as $C_{16}E_8$ or $C_{16}EO_8$] and water is also a typical example exhibiting a phase diagram[5] quite similar (Figure 1) to that of $C_{12}E_6$.[6,7] The $C_{16}E_8$−water system is therefore adequate to examine to what extent the findings obtained in the $C_{12}E_6$−water system are applied.

On the other hand, we have conducted thermodynamic studies on thermotropic cubic mesogens.[8−13] Recently, we proposed the quasi-binary (QB) picture of thermotropic liquid crystals and its application to the thermotropic cubic liquid crystals.[14] The QB picture assumes that the long alkyl chains attached to the mesogenic molecules are highly disordered and serves as intramoleclar solvent ("self-solvent") in liquid crystalline states. This QB picture on thermotropic cubic liquid crystals having no external solvent leads to the conclusion that the neat thermotropic cubic system should be treated together with the lyotropic one in a consistent and unified manner. It is therefore interesting to compare the properties of liquid crystalline phases in lyotropic and thermotropic systems.

In this paper, the results of the precise heat capacity measurements are reported on the lyotropic liquid crystals formed in the $C_{16}E_8$−water binary system utilizing adiabatic calorimetry. Results will be compared with the previous one on the $C_{12}E_6$−water system and some thermotropic systems.

2. Experimental Section

The nonionic surfactant, $C_{16}E_8$ (molar mass: 594.86 g mol^{-1}), was purchased from Nikko Chemical and used for the measurements without further purification.

The lyotropic liquid crystalline samples in the $C_{16}E_8$−water binary system were prepared in the following way. The commercial surfactant was loaded in a sample cell made of gold-plated copper−berilium alloy in a glovebox filled with helium gas (0.1 MPa at room temperature). A necessary amount of degassed pure water was introduced into the cell under a helium

† Contribution No. 79 from the Research Center for Molecular Thermodynamics.

* Corresponding author. E-mail: kazuya@chem.sci.osaka-u.ac.jp.

10.1021/jp0302461 CCC: $25.00
Published on Web 07/01/2003

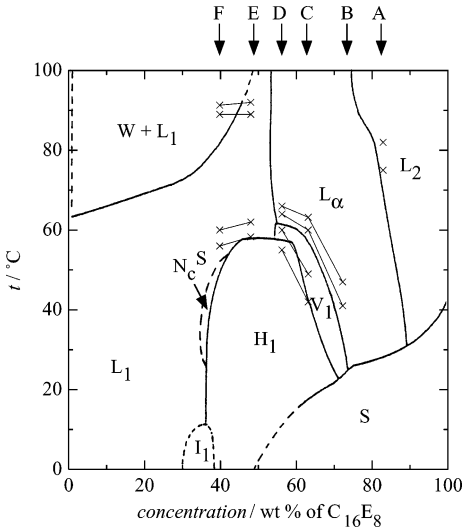

Figure 1. Phase diagram of the $C_{16}E_8$−water system.[5] L_α: lamellar phase. V_1: normal bicontinuous cubic phase. H_1: normal hexagonal phase. I_1: close-packed spherical micelle cubic phase. N_c^S: rod nematic phase. L_1 & L_2: isotropic solution. W: very dilute surfactant solution. S: solid. Phases surrounded by broken lines are reported to be metastable. Arrows over the diagram indicate the concentrations of the samples in this study, the symbols of which are described in Table 1. Crosses are the start and end temperatures of the anomalies in the temperature dependence of the heat capacity.

TABLE 1: Composition of the $C_{16}E_8$−Water Samples Used for the Adiabatic Calorimetry[a]

concn of $C_{16}E_8$, wt %	symbol	total mass	$n(H_2O)/n(C_{12}E_6)$	$n(C_{12}E_6)/n(H_2O)$
82.88	A	8.2360	6.8213	0.14660
72.22	B	3.2323	12.704	0.078711
63.15	C	3.6969	19.264	0.051910
56.22	D	4.1474	25.659	0.038987
48.01	E	4.8615	35.752	0.027971
39.81	F	5.8629	49.917	0.020033

[a] *n* stands for the amount of substance in moles.

atmosphere so that a desired concentration may be prepared. The cell was then sealed with a lid using an indium gasket under a helium atmosphere. The sealed helium gas serves as heat transfer for thermal equilibration inside the cell. Because the result on the first sample (A) showed that the amount loaded was too large for further experiments, the fresh $C_{16}E_8$ from the same batch was newly loaded for succeeding experiments. After the heat capacity measurement was over for a sample with a certain concentration, pure water was added to the cell to prepare another sample with a different concentration. By repeating this procedure, samples with five concentrations were prepared. The composition of the lyotropic liquid crystalline samples is given in Table 1 and indicated by arrows in Figure 1.

After mounting the cell in the calorimeter, the sample was heated once within the one-phase region of the phase diagram to establish homogeneous mixing in the cell. The heat capacity measurement for each sample with different concentrations described above was carried out in the temperature range between 290 and 370 K. The sample contributed more than 50% to the total heat capacity including those of the sample cell and helium gas. A small contribution due to evaporation of water in the closed cell can safely be ignored.

To determine the excess heat capacity in the $C_{16}E_8$−water system, the heat capacity of neat $C_{16}E_8$ was also measured. The mass of the surfactant loaded in the sample cell was 9.6154 g (0.016164 mol) after buoyancy correction. The measurement was carried out between 80 and 373 K.

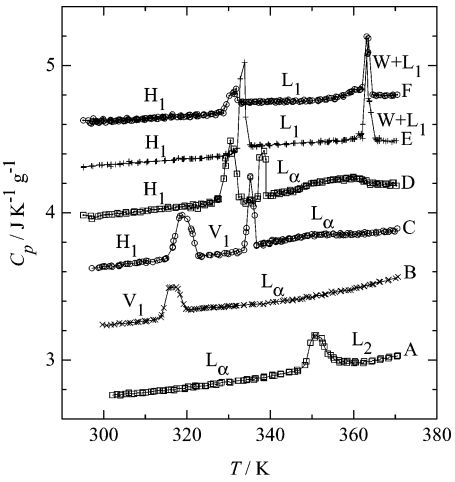

Figure 2. Measured specific heat capacities of six samples in the $C_{16}E_8$−water system. The concentrations of samples (A−F) are described in Table 1. The ordinate is for the sample A. The data of other samples are successively shifted upward by 0.2 J K^{-1} g^{-1}.

The adiabatic calorimeter used is the same as in the previous report on the $C_{12}E_6$−water system.[15] The thermometry was done with a platinum resistance thermometer (S1059, Minco Products, Inc.), the temperature scale of which is based on the ITS-90. The imprecision has not been assessed experimentally but is expected to be better than 1% at worst, judging from the performances of the adiabatic calorimeters constructed by the authors.[16,17]

3. Results

A. Heat Capacity of the $C_{16}E_8$−Water Binary System. Figure 2 shows the heat capacities of the lyotropic liquid crystalline samples with six different concentrations in the $C_{16}E_8$−water binary system. Generally, the specific heat capacity (heat capacity per unit mass) of this binary system increases with decreasing concentration of the surfactant (from A to F in Figure 2).

Taking the reported phase diagram (reproduced in Figure 1) into account, anomalous temperature dependence of the heat capacities, except minor ones discussed later, can reasonably be assigned to known phase transitions, as far as one ignores the fact that the narrow regions of two-phase coexistence are not shown in the original phase diagram.[5] The trapezoidal, relatively wide region of the top of a peak represents the coexistence of two phases. The concentration dependence of the phase transition temperatures observed by the present calorimetry generally coincides with the reported phase diagram[5] as seen in Figure 1.

The time needed for thermal equilibration within the sample cell after each energy input was slightly longer in the transition region than in the normal region. It was about 100 min at the L_α−L_2 transition and about 30−40 min for other transitions.

B. Thermodynamic Quantities at Phase Transitions. Although all known phase transitions in the $C_{16}E_8$−water system are of the first-order,[5] thermal equilibration was established rather in a short time after energy input as described. The temperature dependence of enthalpy was thus determined correctly even in the transition regions.

To determine the thermodynamic quantities associated with the phase transitions, anomalous heat capacities due to phase

TABLE 2: Thermodynamic Properties of the Phase Transitions in the $C_{16}E_8$−Water System[a]

concn (symbol)	H_I		V_I		L_α		L_2		L_1		$W + L_1$	total
82.88 (A)	X		X		O	351	O		X		X	
						986 (2.81)						986 (2.81)
72.22 (B)	X		O	316.4	O		X		X		X	
				506 (1.60)								506 (1.60)
63.15 (C)	O	319.2	O	335.2	O		X		X		X	
		1154 (3.62)		521 (1.56)								1675 (5.18)
56.22 (D)	O	330.4	O	337.9	O		X		X		X	
		1184 (3.59)		497 (1.47)								1681 (5.06)
48.01 (E)	O		X		X		X	333.3	O	363.8	O	
								1013 (3.04)		765 (2.10)		1778 (5.14)
39.81 (F)	O		X		X		X	330.9	O	363.1	O	
								407 (1.23)		788 (2.17)		1195 (3.40)

[a] Concentration is given in wt % of $C_{16}E_8$. O and X under phase designation indicate the presence and absence of the relevant phase, respectively. In the first line for each concentration, the transition temperatures (in K) corresponding to the maxima of the heat capacity curve are given. The enthalpy gain [in J (mol of $C_{16}E_8$)$^{-1}$] and the entropy gain [in J K^{-1} (mol of $C_{16}E_8$)$^{-1}$ in parentheses] are given in the second line.

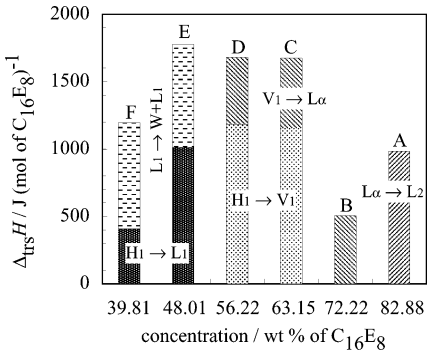

Figure 3. Cumulative transition enthalpies of six samples in the $C_{16}E_8$−water system. The concentrations of samples (A−F) are described in Table 1.

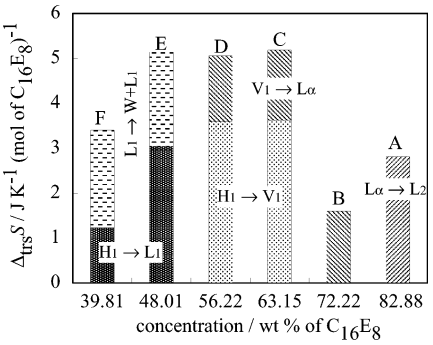

Figure 4. Cumulative transition entropies of six samples in the $C_{16}E_8$−water system. The concentrations of samples (A−F) are described in Table 1.

transitions were separated and integrated with respect to T and ln T, yielding the enthalpy and entropy of transition, respectively. The resulting quantities are summarized in Table 2. These enthalpies and entropies are given on the basis of a mole of $C_{16}E_8$.

Figures 3 and 4 show the cumulative transition enthalpies and entropies of the $C_{16}E_8$−water binary system as a function of concentration, respectively. As clearly seen in these figures, for the samples with higher concentrations of $C_{16}E_8$ (samples B−D), which exhibits either two or three kinds of liquid crystalline phases (H_1, V_1, and L_α), the enthalpy and entropy of transitions between H_1 and V_1 phases and those between V_1 and L_α phases remain almost constant independently of the concentration. The constancy implies that their higher order structures are mainly constructed by $C_{16}E_8$ or a $C_{16}E_8$−water "complex" with a fixed composition. Similar constancy was

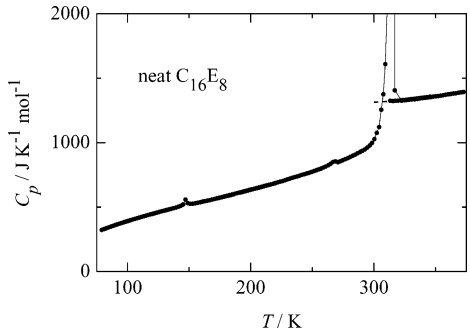

Figure 5. Measured molar heat capacities of neat $C_{16}E_8$. An extrapolation from the liquid region is shown by a dotted curve.

already recognized in the $C_{12}E_6$−water system for the same phase transitions.[4]

On the other hand, at the phase transition between H_1 and L_1, the enthalpy and entropy are smaller in the sample with a smaller concentration of $C_{16}E_8$. Because the apparent constancy of the enthalpy and entropy of H_1−V_1 and V_1−L_α transitions implies the same state of the liquid crystalline phases, the decrease in the total enthalpy and entropy probably results from a change in the isotropic micellar solution (L_1 phase).

C. Heat Capacity of $C_{16}E_8$ Surfactant. To discuss the interaction between $C_{16}E_8$ and water molecules, excess heat capacity should be compared. The calculation of the excess heat capacity requires the heat capacities of liquid $C_{16}E_8$ and water. Figure 5 shows the molar heat capacities of neat $C_{16}E_8$ surfactant. Small anomalies are recognized at 147 and 269 K, which would be due to phase transitions between solid phases.

As clearly seen in the phase diagram of the $C_{16}E_8$−water binary system (Figure 1), $C_{16}E_8$ melts above room temperature. The heat capacity measurement from 80 K revealed the presence of a large tail below the melting temperature extending down to about 250 K. The peak of the heat capacity due to the melting is the highest at 316 K (43 °C), and this anomaly ranges over wide temperatures both below and above the peak (250−320 K). It has been well established that on the basis of adiabatic calorimetry one can determine precisely the temperature of fusion and the purity of the sample if one could wait until thermal equilibration between the two phases (solid and liquid) for a long time under an excellent adiabatic condition. A preliminary trial to see thermal equilibrium in the melting region showed that the time required for thermal equilibration was longer than a day. As the interest lies in thermal behavior of thermotropic liquid crystalline states, the thermal equilibration in the melting region was abandoned. The data in this region

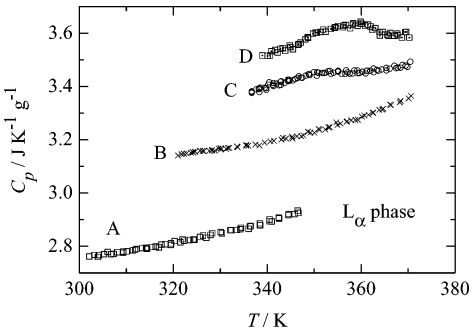

Figure 6. Enlarged plot of heat capacities of the L_α phase in the $C_{16}E_8$−water system.

are, therefore, regarded as approximate ones. It should be noted, however, that the integrated enthalpy is as reliable as the heat capacity data outside the melting region. The enthalpy of fusion at 316 K was determined as 130.4 kJ mol^{-1} including the contributions of the low-temperature tails.

Although the melting temperature of $C_{16}E_8$ is around 316 K, we need the heat capacity data of liquid $C_{16}E_8$ down to 290 K, from which the calorimetric measurements have been done for the $C_{16}E_8$−water binary system. However, the liquid state was not supercooled to so low as 290 K. Heat capacity of the liquid was only possible to be measured above 312 K.

4. Discussion

A. Anomaly Related to Perforation Fluctuation Layer State. In the related systems consisting of water and $C_{16}E_6$ or $C_{16}E_7$, the formation of the perforation fluctuation layer (PFL) states has been suggested in the L_α phase just above the V_1−L_α transition. The PFL state was assumed to be dynamically fluctuating inside the L_α phase in thermal equilibrium for the latter system.[18,19] The presence of a small excess heat capacity was also suggested from the differential scanning calorimetric (DSC) result.[18] On the other hand, the PFL state was assumed to be a distinct phase (L_α^H) for the former system.[20] It is, however, noted that no thermodynamic evidence has been reported to certify the existence of the L_α^H−L_α transition.

The heat capacities of the L_α phases are shown in an enlarged scale in Figure 6. There is a sluggish hump centered around 350 K in the result of sample C. A similar anomaly can also be recognized around 325 K for sample B. Their shape seems similar to that by DSC reported previously.[18] The location of the anomaly in the phase diagram suggests that the excess heat capacity with the hump found in sample C is related to the formation of the PFL state in the $C_{16}E_8$−water system, though no experimental evidence has been reported as far as we know. It is noted that similar broad hump can be recognized in the previous paper on the $C_{12}E_6$−water system.[4]

In sample D, on the other hand, a trapezoidal hump exists between 350 and 360 K. Such a shape can be rationalized if the two-phase coexistence due to phase separation is assumed to exist. The location of the hump again suggests that the hump be related to the formation of the PFL state. The most naive intuition thus leads to the assumption of two-phase coexistence between the PFL *phase* (or L_α^H phase) and the L_α phase, which is assumed to be essentially defect-free.

B. Thermodynamic Quantities at Phase Transitions in $C_{16}E_8$−Water and $C_{12}E_6$−Water Systems. The thermodynamic quantities at phase transitions determined by the present study on the $C_{16}E_8$−water system and by the previous one on the $C_{12}E_6$−water system[4] reveal that the entropies (or enthalpies) of the H_1−V_1 and V_1−L_α transitions are independent of (or weakly dependent on) concentration whereas that of the H_1−L_1 transition strongly depends on it. The constancy of the entropy (enthalpy) of transition implies that their higher order structures are mainly constructed by surfactant or a surfactant−water "complex" with a fixed composition.

The entropy of the H_1−V_1 transition is ca. 3.6 J K^{-1} (mol of $C_{16}E_8$)$^{-1}$ in the present system and 2.9−3.1 J K^{-1} (mol of $C_{12}E_6$)$^{-1}$ in the $C_{12}E_6$−water system.[4] Their ratio is 1.24, which is roughly equal to the ratios (1.32) of the numbers of atoms in a surfactant molecule and/or the surfactant molar mass. Namely, the entropy of transition increases in proportion to the size of surfactant. This proportionality supports the hypothesis that their higher order structures are mainly constructed by surfactant or a surfactant−water "complex" with a fixed composition. Because the molecule of $C_{16}E_8$ is proportionally enlarged in comparison to $C_{12}E_6$, it is impossible from this comparison to assess which part, hydrophilic or hydrophobic, is responsible for structure building. It is widely accepted,[2] however, that the H_1−V_1 transition is driven by the decrease in interfacial curvature due to the reduced hydration of the hydrophilic group. The proportional increase of entropy of transition to the size of the hydrophilic group is consistent with this common understanding.

In contrast to the H_1−V_1 transition, the entropy of the V_1−L_α transition is commonly ca. 1.6 J K^{-1} (mol of surfactant)$^{-1}$ in the $C_{16}E_8$−water (56−72 wt %), $C_{12}E_6$−water (63−70 wt %),[4] and $C_{16}E_7$−heavy water (55 wt %, by commercial DSC)[18] systems. The constancy suggests the presence of some universal meaning of the magnitude.

The contrasting dependence of entropy of transition on surfactant size is hard to rationalize as far as the physical significance of the common aggregation mode in the H_1 and V_1 phases (rod micelle) and the different one (sheet) in the L_α phase are assumed. As is well-known, however, that the V_1 phase can alternatively be described by the presence of Gyroid,[21] a triply periodic minimal surface (TPMS). If the Gyroid is assumed to be of primary importance in the V_1 phase, the behavior of the entropy of transition can be understood as follows: Under this assumption, the basic aggregation mode of physical relevance is commonly of sheet in the V_1 and L_α phases whereas it is cylinder in the H_1 phase. The reconstruction from cylinder to sheet requires the destruction of the starting aggregation mode of the H_1 phase, in which the hydrophilic part of surfactant may be assumed to be mainly involved. Once the sheet aggregation is established, the transition between the V_1 and L_α phases only accompanies a universal magnitude of entropy of transition because this transition requires only a change in topology (connectivity) of the sheet. In the language of the surfactant parameter and surface curvature, the change in surfactant parameter upon the H_1−V_1 transition originates in the reducing hydration of the hydrophilic part, resulting in the change in surface curvature corresponding to the cylinder to the Gyroid.

C. Excess Heat Capacity of the $C_{16}E_8$−Water Binary System. The excess heat capacity of the $C_{16}E_8$−water system, which is defined as the quantity beyond the sum of heat capacities of pure $C_{16}E_8$ and water, would provide important information concerning their interactions and the structure formation caused by them. The heat capacities of liquid $C_{16}E_8$ and water were therefore subtracted from the observed values for the lyotropic liquid crystalline samples. The heat capacity of liquid $C_{16}E_8$ was experimentally determined in this study above 312 K, below which the temperature dependence of the heat capacity is smoothly extrapolated, as shown by a dotted

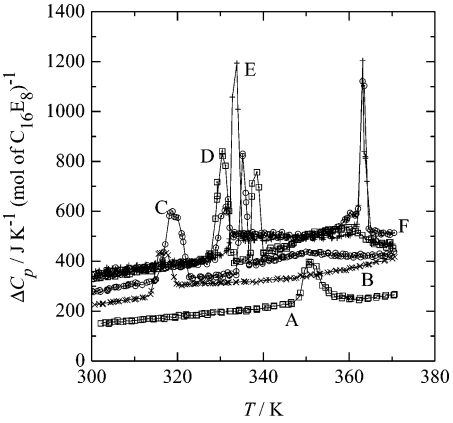

Figure 7. Excess heat capacities of six samples in the $C_{16}E_8$−water system calculated on per mol of $C_{12}E_6$ basis. The concentrations of samples (A−F) are described in Table 1. The symbols are the same as those in Figure 2.

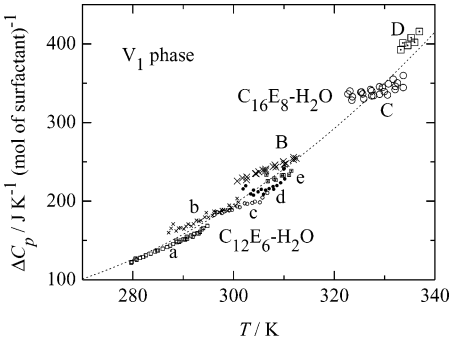

Figure 8. Excess heat capacities of the V_1 phase in the $C_{16}E_8$−water and $C_{12}E_6$−water[4] systems calculated on per mol of surfactant basis. The concentrations of the samples of the $C_{16}E_8$−water system (B−D) are described in Table 1. The concentration of the samples of the $C_{12}E_6$−water system are (a) 69.54, (b) 67.56, (c) 64.94, (d) 62.80, and (e) 60.78 wt %. The symbols for the samples of the $C_{16}E_8$−water system are the same as those in Figure 2. A "master curve" is drawn by a dotted curve.

curve in Figure 5. On the other hand, reliable heat capacity of liquid water can be found in the literature.[22]

The resulting excess heat capacities are shown in Figure 7. The heat capacity caused by the interactions between solute and solvent is positive by ca. 10% of the total heat capacity. Figures 7 show the excess heat capacities in units of mole of surfactant. In a previous paper on the $C_{12}E_6$−water system,[4] plots in different units (mole of surfactant, water, and mixture) are compared, and the plot in the present unit (mole of surfactant) is shown to be more adequate to clarify the aggregation mechanism, as shown in the discussion on the entropies of transition.

The excess heat capacity of the L_α, L_1, and L_2 phases strongly depends on the concentration. This is easily expected for the L_1 and L_2 phases because they are uniform mixtures, and the tendency is rationalized by assuming the water molecules penetrate into the bilayer in the L_α phase. The concentration dependence of the excess heat capacity of both phases is normalized by neither the amount of water nor the mole fraction of mixture. The interaction between $C_{16}E_8$ and water molecules certainly depends on the concentration in these phases.

In a previous paper,[4] it was shown that the neighboring H_1 and V_1 phases in the $C_{12}E_6$−water system show "master curves" of heat capacity if presented in the unit of mole of surfactant. In the present $C_{16}E_8$−water system, such a tendency can be recognized only for the V_1 phase, as shown in Figure 8, where the excess heat capacities of the V_1 phase in the $C_{12}E_6$−water system are also shown. As described in the last section, the contrasting dependence of entropies of transition on the surfactant size can be rationalized by assuming the primary importance of a TPMS (Gyroid) to describe the aggregation state of the V_1 phase.[21] If this is the case, a single "master curve" may be drawn while the difference in surfactant is ignored, as shown in Figure 8.

D. Comparison with Thermotropic Systems. The QB picture of thermotropic liquid crystals recently proposed by us[14] leads to the conclusion that the neat thermotropic cubic system should be treated together with a lyotropic one in a consistent and unified manner. Here, such a treatment is intended.

The QB picture naturally relates the smectic phase in thermotropics to the lamellar phase in lyotropics in addition to the correspondence between the cubic phase with space group *Ia*3*d* and the V_1 phase. Both the smectic (Sm) phase and L_α phase are characterized by flat surfaces whereas the cubic *Ia*3*d* phase and V_1 phase by Gyroid (a TPMS). Geometries of the

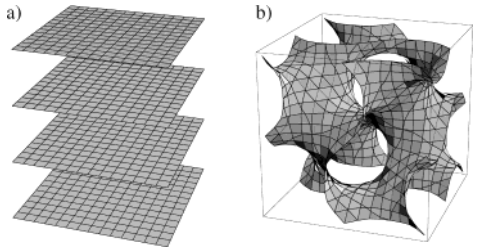

Figure 9. Surface geometries characterizing the L_α and SmC phases (a) and the cubic *Ia*3*d* phase (b).

characteristic surfaces are shown in Figure 9. In neat thermotropic systems, the surface is considered to consist of mesogenic cores with vertical orientation to the surface.[14]

Due to the 3D connectivity (3D periodicity), structures characterized by TPMS are expected to be more stiff than flat surfaces.[23] Lyotropic cubic phases are often called "viscous liquids" because of their viscous property without optical anisotropy. On the other hand, the viscoelastic property of neat thermotropic mesogen ANBC (4′-*n*-alkoxy-3′-nitrobiphenyl-4-carboxylic acid) reported previously[24,25] shows that the cubic phases (with space groups *Ia*3*d* and *Im*3*m*) are much stiffer than the neighboring SmC phases.

The fluctuation of the surface is expected to be more strongly suppressed in TPMS phases also due to 3D connectivity of the surfaces. Indeed the heat capacity, which is proportional to enthalpy fluctuation, of the V_1 phase is smaller than that of the L_α phase in all samples in the present study, as clearly exemplified by the result on sample B in Figure 2. A smaller heat capacity of the V_1 phase has been observed also in the $C_{12}E_6$−water system in a previous paper.[4] Besides, the thermotropic cubic phases exhibit smaller heat capacities than neighboring liquid crystalline phases.[10,11,13,26] The hypothesis of the suppressed fluctuation by the 3D connectivity, therefore, works well for the available heat capacity data.

The degree of fluctuation should also be reflected in entropy. The thermodynamic analysis showed that the aggregation states in the cubic *Ia*3*d* phases in ANBC and BABH [1,2-bis(4-*n*-alkoxybenzoyl)hydrazine] are essentially the same despite the reversed order of phase sequence (SmC phase → cubic *Ia*3*d* phase in ANBC whereas cubic *Ia*3*d* phase → SmC phase in BABH on heating),[11,13] which is caused by the competing roles of the molecular core and alkyl chains in stabilizing the cubic phases. According to the structural model of the *Ia*3*d* phase

based on the QB picture,[14] the Gyroid is formed by the sheet consisting of the molecular cores, of which the contribution to the entropy of the SmC−cubic *Ia*3*d* phase transition might be regarded as the entropy of the ideal (fictive) phase transition between the Gyroid and flat surface "phases." The analysis[11,13] showed that this core contribution is negative, indicating the Gyroid "phase" has a smaller entropy than the flat surfaces "phase." This is in accordance with the expectation based on the suppressed fluctuation of TPMS. On the other hand, the V_1 phase is located in the low-temperature side of the L_α phase in C_nE_m−water systems. This automatically guarantees that the V_1 phase has a smaller entropy than the L_α phase. Although the entropy of transition may contain other contributions, as in the case of thermotropics described above, its "universal" magnitude, as implied by the same value in the $C_{16}E_8$−water and $C_{12}E_6$−water[4] systems, suggests that this entropy of transition comes from the reconstruction of the surface discussed in a previous section. In lyotropic systems where the V_1 phase locates at the high-temperature side of the L_α phase, the transition sequence is usually understood by considering the change in surface curvature due to the enhanced disorder of hydrophobic alkyl chains with increasing temperaure.[21] It is noted that the phase sequence can be alternatively rationalized as an entropy contribution of alkyl chains as in thermotropic ones, though no supporting data from thermodynamics is available yet.

Thermotropic cubic phases of ANBC and BABH commonly have a larger volume (smaller density) than the neighboring SmC phases, as evidenced by the different sign of $(dT_{trs}/dp) = \Delta_{trs}V/\Delta_{trs}S$ (Clapeyron's equation),[27−29] despite the reverse phase sequence with respect to temperature. This suggests that in these theromtropic systems the net volume of the cubic phase be primarily determined not by the highly disordered alkyl chains but by the densely packed and 3D connected TPMS. The V_1 phase in the $C_{12}E_6$−water system has a larger density than the neighboring L_α phase,[30] in contrast to the above thermotropic systems, though some lyotropic cubic phases appearing at the high-temperature side of a lamellar phase have been reported to have a smaller density.[31] Consequently, the parallel discussion does not hold in lyotropic and thermotropic cubic phases for their volume (density). The difference probably originates in the property of the physical TPMS: Two sides of the TPMS can take relative flow in lyotropic systems whereas such flow is impossible in the thermotropic systems under discussion because a single particle (molecule or carboxylic acid dimer) bridges two sides.

E. Entropy and Periodicity of TPMS. Qualitative comparison of the lyotropic and thermotropic systems is consistent with the naive intuition described in the last section. Quantitative interpretation is, on the other hand, only at a starting point. According to the thermodynamic analysis on the thermotropic systems, for example, the contribution of molecular cores to the entropy of SmC → cubic *Ia*3*d* transition is about $-(1 \pm 0.5)R$ ($R = 8.31$ J K^{-1} mol^{-1}: gas constant), if the dimerized molecular core is assumed as a unit particle.[11,13] On the other hand, the corresponding entropy of transition is 1.6 J K^{-1} (mol of surfactant)$^{-1}$ [or 3.2 J K^{-1} (mol of "dimer")$^{-1}$ for comparison] in the present lyotropic systems.[4,18] Prior to concluding the paper, in this section, the importance of understanding the entropy of TPMS and related "phases" is briefly discussed.

Each TPMS is characterized by its global connectivity besides its local properties such as zero mean curvature and negative Gaussian curvature. Even so, in fact, three TPMS's (Gyroid, Schwarz's P and D surfaces) [and even their smooth, nonperiodic "mixture" (mosaic)] have the same stability because they are related by Bonnet transformation.[21] The importance of the global connectivity will put a striking aspect on enumerating the number of microscopic states (or equivalently, entropy) for TPMS with respect to conventional aggregation states. As to a question whether a particle is in a "correct" state, for example, the answer could be available only after viewing over more than a length scale of lattice periodicity for TPMS whereas it is certainly determined from states of several neighboring particles for, e.g., spin systems. This situation suggests that the entropy discriminate the most stable one from other possible TPMS's. Furthermore, taking into account the crystallization of hard spheres[32] where the entropy is only a driving factor to bring crystallization, it is even anticipated that the entropy is a primary driving force of the periodicity of TPMS.

The most naive assumption is to assign a common amount of entropy to a cubic unit cell, a building block of the 3D periodic structure. Because the numbers of surfactant molecules in the cubic phases of $C_{12}E_6$−water and $C_{16}E_7$−heavy water systems are ca. 1400 in common,[18,33] the magnitude 1400×1.6 J K^{-1} (mol of surfactant)$^{-1}$ $\approx 2.2 \times 10^3$ J K^{-1} (mol of cell)$^{-1}$ may be assigned as the entropy difference between the Gyroid and flat surface phases ($-\Delta S_{flat->Gyroid}$) here.

Although the translational degree of freedom for the relative motion (flow) of two sides of a sheet (interface) is certainly different in lyotropic and thermotropic systems, as described previously, this degree of freedom may be assumed to be equally active for the lyotropic systems (inactive for the thermotropic systems) in both the Gyroid and flat surface phases. Assuming the entropy difference on the unit cell basis, therefore, the entropy of the SmC−cubic *Ia*3*d* phase transition may be analyzed in a framework of the QB picture as $\Delta_{trs}S = \Delta S_{flat->Gyroid}/Z + (n - n_{core})\Delta S_{chain}$, where Z is the number of molecules in a cubic unit cell and n_{core} is the number of methylene groups included in the effective mesogenic core. Indeed, this formula assuming $\Delta S_{flat->Gyroid} = 2.2 \times 10^3$ J K^{-1} (mol of cell)$^{-1}$ can reproduce the chain-length dependence of $\Delta_{trs}S$ in ANBC. More experimental information on other systems is, however, necessary to continue the discussion along this direction.

If the unit cell of the cubic phase behaves like a unit "particle" having a constant entropy, which may be different from system to system, an interesting behavior is expected. According to the thermodynamic inequality $(\partial S/\partial T)_v \geq 0$,[34] the cell parameter should be a nonincreasing function of temperature because the only way to increase the entropy of the system consisting of TPMS unit cells having a constant entropy is to increase the number of cells. This does not mean a negative thermal expansion but a decreasing size of the cubic unit cell upon heating with a decreasing number of molecules in a cell. Such behavior is really reported for thermotropic ANBC[35] and some lyotropic systems,[31,36,37] though the behavior can alternately be interpreted as being due to the increased curvature of the surface (interface) by a larger thermal expansion of the alkyl chains. In this context, studies are interesting on C_nE_m−water systems and thermotropic BABH, in both of which the cubic phases locate below the lamellar or smectic phases.

It is hard (and probably meaningless) at this stage to discuss further without experimental and/or theoretical basis. This is left for future theoretical studies. On the experimental side, enumeration of entropies on many TPMS's and their comparison are a promising way to proceed.

5. Summary and Conclusion

The heat capacities of the binary system consisting of a nonionic surfactant $C_{16}E_8$ and water, and that of neat $C_{16}E_8$ were

precisely measured as a function of temperature by adiabatic calorimetry. The temperature and the concentration cover the range where lyotropic liquid crystals are formed.

The anomalous temperature dependence associated with the PFL formation was detected in the L_α phase. The possible presence of the PFL *phase* as a definite thermodynamic phase and the coexistence with the normal L_α phase in a certain temperature (concentration) range are also suggested from the shape of the anomaly.

The enthalpy and entropy of transitions were determined. The enthalpy and entropy gains at the phase transitions between liquid crystalline phases were essentially constant if compared per mol of $C_{16}E_8$ basis. This finding implies that the higher order structure in the liquid crystalline phases in this system is mainly built by $C_{16}E_8$ molecules with a fixed amount of water. The excess heat capacities were estimated to be positive over whole temperature and concentration ranges.

Comparison of entropies of transition reveals that one for the V_1-L_α transition is the same for some similar surfactants irrespective of its concentration whereas one for the H_1-V_1 transition increases in proportion to the surfactant size. This can be rationalized if the crucial (physical) importance is assumed for the Gyroid to characterize the V_1 phase. The excess heat capacities of the V_1 phases of $C_{16}E_8$−water and $C_{12}E_6$−water systems show a "master curve" if presented per mol of surfactant basis.

Suppression of fluctuation by 3D connectivity of TPMS is shown to work in both the lyotropic and thermotropic cubic phases. Importance of understanding the entropy of TPMS and related phases is briefly discussed in relation to the origin of the 3D periodicity of physical TPMS phases.

Acknowledgment. This work was partially supported by a Grant-in-Aid for Scientific Research (A) (11304050) from the Ministry of Education, Science, Sports, and Culture, Japan. We express our thanks to Prof. T. Kato at Tokyo Metropolitan University and Prof. S. Kutsumizu at Gifu University for their stimulating discussion.

References and Notes

(1) Demus, D.; Goodby, J.; Gray, G. W.; Spiess, H.-W.; Vill, V. *Handbook of Liquid Crystals, Vol. 3: High Molecular Weight Liquid Crystals*; Amphiphilic Liquid Crystals; Wiley-VCH: Weinheim, 1998; Part 3.

(2) Borisch, K.; Diele, S.; Göring, P.; Muller, H.; Tschierske, C. *Liq. Cryst.* **1997**, *22*, 427.

(3) Israelachvili, J. N.; Mitchell, D. J.; Ninham, B. W. *J. Chem. Soc., Faraday Trans. 2* **1976**, *72*, 1525.

(4) Nishizawa, M.; Saito, K.; Sorai, M. *J. Phys. Chem. B* **2001**, *105*, 2987.

(5) Corcoran, J.; Fuller, S.; Rahman, A.; Shinde, N. N.; Tiddy, G. J. T.; Attard, G. S. *J. Mater. Chem.* **1992**, *2*, 695.

(6) Clunie, J. S.; Goodman, J. F.; Symons, P. C. *Trans. Faraday Soc.* **1969**, *65*, 287.

(7) Mitchell, D. J.; Tiddy, G. J. T.; Waring, L.; Bostock, T.; McDonald, M. P. *J. Chem. Soc., Faraday Trans. 1* **1983**, *79*, 975.

(8) Saito, K.; Sato, A.; Sorai, M. *Liq. Cryst.* **1998**, *25*, 525.

(9) Morimoto, N.; Saito, K.; Morita, Y.; Nakasuji, K.; Sorai, M. *Liq. Cryst.* **1999**, *26*, 219.

(10) Sato, A.; Saito, K.; Sorai, M. *Liq. Cryst.* **1999**, *26*, 341.

(11) Sato, A.; Yamamura, Y.; Saito, K.; Sorai, M. *Liq. Cryst.* **1999**, *26*, 1185.

(12) Saito, K.; Shinhara, T.; Sorai, M. *Liq. Cryst.* **2000**, *27*, 1555.

(13) Saito, K.; Shinhara, T.; Nakamoto, T.; Kutsumizu, S.; Yano, S.; Sorai, M. *Phys. Rev. E* **2002**, *65*, 031719.

(14) Saito, K.; Sorai, M. *Chem. Phys. Lett.* **2002**, *366*, 56.

(15) Nishizawa, M.; Asahina, S.; Saito, K.; Sorai, M. Unpublished work.

(16) Sorai, M.; Kaji, K.; Kaneko, Y. *J. Chem. Thermodyn.* **1992**, *24*, 167.

(17) Yamamura, Y.; Saito, K.; Saitoh, H.; Matsuyama, H.; Kikuchi, K.; Ikemoto, I. *J. Phys. Chem. Solids* **1995** *56*, 107.

(18) Imai, M.; Kawaguchi, A.; Saeki, A.; Nakaya, K.; Kato, T.; Ito, K.; Amemiya, Y. *Phys. Rev. E* **2000**, *62*, 6865.

(19) Minewaki, K.; Kato, T.; Yoshida, H.; Imai, M.; Ito, K. *Langmuir* **2001**, *17*, 1864.

(20) Fairhurst, C. E.; Holmes, M. C.; Leaver, M. S. *Langmuir* **1997**, *13*, 4964.

(21) Hyde, S.; Andersson, A.; Larsson, K.; Blum, Z.; Landh, T.; Lidin, S.; Ninham, B. W. *The Language of Shape*; Elsevier Science: Amsterdam, 1997.

(22) Chase, Jr. M. W. *NIST-JANAF Themochemical Tables*, 4th ed.; J. Phys. Chem. Ref. Data Monograph 9; American Chemical Society: Washington, DC, 1998; p 1.

(23) Eriksson, J. C.; Ljunggren, S. *J. Colloid Interface Sci.* **1994**, *167*, 227.

(24) Yamaguchi, T.; Yamada, M.; Kutsumizu, S.; Yano, S. *Chem. Phys. Lett.* **1995**, *240*, 105.

(25) Kutsumizu, S.; Yamaguchi, T.; Kato, R.; Yano, S. *Liq. Cryst.* **1999**, *26*, 567.

(26) Ema, K.; Yao, H.; Takanishi, Y.; Takezoe, H.; Kusumoto, T.; Hiyama, T.; Yoshizawa, A. *Liq. Cryst.* **2002**, *29*, 221.

(27) Shankar, D. S.; Prasad, S. K.; Prasad, V.; Kumar, S. *Phys. Rev. E* **1999**, *59*, 5572.

(28) Maeda, Y.; Cheng, G.-P.; Kutsumizu, S.; Yano, S. *Liq. Cryst.* **2001**, *28*, 1785.

(29) Maeda, Y.; Saito, K.; Sorai, M. *Liq. Cryst.*, in press.

(30) Mita, S.; Kondo, S. *J. Chem. Soc., Faraday Trans.* **1995**, *91*, 319.

(31) Czeslik, C.; Winter, R.; Rapp, G.; Bartels, K. *Biophys. J.* **1995**, *68*, 1423.

(32) Mau, S.-C.; Huse, D. A. *Phys. Rev. E* **1999**, *59*, 4396.

(33) Clerc, M.; Levelut, A. M.; Sadoc, J. F. *J. Phys. II Fr.* **1991**, *1*, 1263.

(34) Landau, L. D.; Lifshitz, E. M. *Statistical Physics*, 3rd ed.; Pergamon Press: New York, 1980; Part 1.

(35) Kutsumizu, S.; Morita, K.; Ichikawa, T.; Yano, S.; Nojima, S. *Liq. Cryst.* **2002**, *29*, 1447.

(36) Erbes, L.; Czeslik, C.; Hahn, W.; Rappolt, M.; Rapp, G.; Winter, R. *Ber. Bunsen-Ges. Phys. Chem.* **1994**, *98*, 1287.

(37) Qiu, H.; Caffrey, M. *Biomaterials* **2000**, *21*, 223.